CAN WE IGNORE P-WAVE VELOCITY IN FULL WAVEFORM INVERSION OF SHALLOW SEISMIC RAYLEIGH WAVES?

L. Groos, M. Schäfer, T. Forbriger and T. Bohlen

email: *Lisa.Groos@kit.edu*

keywords: *2D full waveform inversion, surface waves*

ABSTRACT

We perform reconstruction tests to investigate the influence of the initial P-wave velocity model on the reconstruction of the S-wave velocity model in a full waveform inversion (FWI) of shallow seismic surface waves. In the reconstruction tests we use a known subsurface model to simulate an observed dataset. This dataset is afterwards inverted by a FWI where we vary the handling of the P-wave velocity model in the inversion. The results of the inversion tests show that the P-wave velocity model has a significant bias on the reconstruction of the S-wave velocity model. In our tests the true P-wave velocity model consists of a layer over a halfspace. Using a wrong layer over halfspace model (velocities as well as the depth of the discontinuity deviate from the true P-wave velocity model) and keeping this model fixed in the inversion causes strong artefacts in the obtained S-wave velocity model. The reconstruction of the S-wave velocity becomes better if we also invert for P-wave velocity. However, we are not able to reconstruct the true P-wave velocity model.

INTRODUCTION

We aim for the full waveform inversion (FWI) of recorded shallow seismic Rayleigh waves. The inversion of shallow seismic Rayleigh waves is very attractive for geotechnical investigations because they can be easily excited by a hammer blow and have a high sensitivity to the shear wave velocity in the first few metres of the subsurface. Furthermore, Rayleigh waves have a better signal to noise ratio compared to body waves and can be used to investigate sites with low velocity zones which cannot be done with refracted body waves. There are established methods to invert Rayleigh waves (e. g. inversion of dispersion curves or wavefield spectra (Forbriger, 2003)) but all these methods assume 1D subsurface structures. To overcome this limitation we apply FWI to shallow seismic Rayleigh waves. Romdhane et al. (2011) as well as Tran and McVay (2012) have shown first successful applications of a FWI of Rayleigh waves which show the high potential of this method.

Because of the high sensitivity of surface waves to the S-wave velocity we focus on the inversion of this model parameter. However, for the forward modeling during the inversion we also have to assume a P-wave velocity model and a strategy how to handle it. We can either invert also for the P-wave velocity or we can keep it constant in the inversion. In the inversion of dispersion curves it is commonly assumed that the dispersion properties are mainly affected by the vertical variation of S-wave velocity. P-wave velocity is thus neglected. In this report we analyse if ignoring P-wave velocity is also justified in the FWI where also amplitudes of the Rayleigh waves are taken into account. We present results of reconstruction tests in which we use a known subsurface model as true model and simulate observed data with this model. Afterwards the simulated observed data are inverted in a FWI and the resulting S-wave velocity model is analysed. As we know the true subsurface model in these tests we can investigate the reconstruction of the S-wave velocity model by FWI directly and therefore, we call these tests in the following reconstruction

tests.

The report is organized as follows. First we introduce the true model and the acquisition geometry which we use for the reconstruction tests. Afterwards we describe the inversion strategy and present results of four different reconstruction tests.

TRUE MODEL AND ACQUISITION GEOMETRY

For the reconstruction tests we use the one dimensional model shown in Figure 1. It is derived from a field dataset which was acquired on a predominantly depth dependent structure at Rheinstetten near Karlsruhe (Germany) by a joint inversion of wavefield spectra and first arrival travel times of P-waves (Forbriger, 2003). The P-wave velocity model (Figure 1a and d) consists of a layer over a halfspace with a strong discontinuity at 6.3 m depth and is mainly constrained by first arrival P-wave travel times. The S-wave velocity model (Figure 1b and e) consists of a steep gradient in the topmost metre, below the gradient decreases. Such a gradient in the first metres of the S-wave velocity model is typical for unconsolidated sediments (Bachrach et al., 2000) and is often observed in shallow seismics. In contrast to the P-wave velocity model the discontinuity at 6.3 m depth is hardly present in the S-wave velocity model and is therefore interpreted as ground water table. The S-wave velocity model is constrained by the inversion of wavefield spectra. The density model (Figure 1c) is not well constrained by the field data and consists of three layers with density values between $1700\,\mathrm{kg/m^3}$ and $2000\,\mathrm{kg/m^3}$. As observed data we simulate viscoelastic seismograms with a quality factor of approximately 20 for both, P-waves as well as S-waves. For the simulation we use a 2D Finite Difference scheme in the time domain where the rheological model is implemented by a generalized standard linear solid (GSLS) with three relaxation mechanisms (Robertsson et al., 1994; Bohlen, 2002). The approximation of a constant quality factor is satisfactory in the frequency band between 10 Hz and 70 Hz which is used in the inversion. The acquisition geometry consists of eight vertical force sources with a spacing of 10 m (see red stars in Figure 1d and e) and 63 two component receivers (vertical and radial component) which are located between the sources with a spacing of 1 m.

INVERSION SETUP

We applied a 2D elastic FWI using the adjoint method in the time domain (Tarantola, 1988; Mora, 1987). The forward modeling is done with Finite Differences in the time domain (Bohlen, 2002). The code was developed by Köhn (2011) and uses a preconditioned conjugate gradient method. As misfit function we use the least squares misfit of the normalized wavefields

$$E = \frac{\sum_i^{n_s}\sum_j^{n_r}\sum_k^{n_c}\left|\hat{\mathbf{s}}_{i,j,k}-\hat{\mathbf{d}}_{i,j,k}\right|^2}{\sum_i^{n_s}\sum_j^{n_r}\sum_k^{n_c}\left|\hat{\mathbf{d}}_{i,j,k}\right|^2} = \frac{\sum_i^{n_s}\sum_j^{n_r}\sum_k^{n_c}\left|\hat{\mathbf{s}}_{i,j,k}-\hat{\mathbf{d}}_{i,j,k}\right|^2}{n_s\cdot n_r\cdot n_c} \tag{1}$$

suggested by Choi and Alkhalifah (2012) where the sum over i denotes the sum over the n_s sources, the sum over j denotes the sum over the n_r receivers and the sum over k denotes the sum over the n_c components and $\hat{\mathbf{s}}_{i,j,k} = \mathbf{s}_{i,j,k}/|\mathbf{s}_{i,j,k}|$ and $\hat{\mathbf{d}}_{i,j,k} = \mathbf{d}_{i,j,k}/|\mathbf{d}_{i,j,k}|$ are the normalized synthetic and observed displacement seismograms, respectively. In comparison to the norm suggested by Choi and Alkhalifah (2012) we added a normalization factor to the misfit function to scale it with the energy of the observed dataset. This misfit norm can be also formulated as a zero lag cross correlation of two normalized signals (Choi and Alkhalifah, 2012). We use the misfit function of equation (1) because it is not sensitive to an amplitude decay with offset. Therefore, far and near offset traces similarly contribute to the misfit.

We investigate two kinds of reconstruction tests. In two tests we fixed the initial P-wave velocity model and only invert for S-wave velocity and density and in the other two tests we invert for all three elastic parameters, P-wave velocity, S-wave velocity and density. In all tests we do not invert for viscoelastic parameters like Q values or relaxation frequencies. We use viscoelastic forward modeling with the correct Q values of 20 in the inversion.

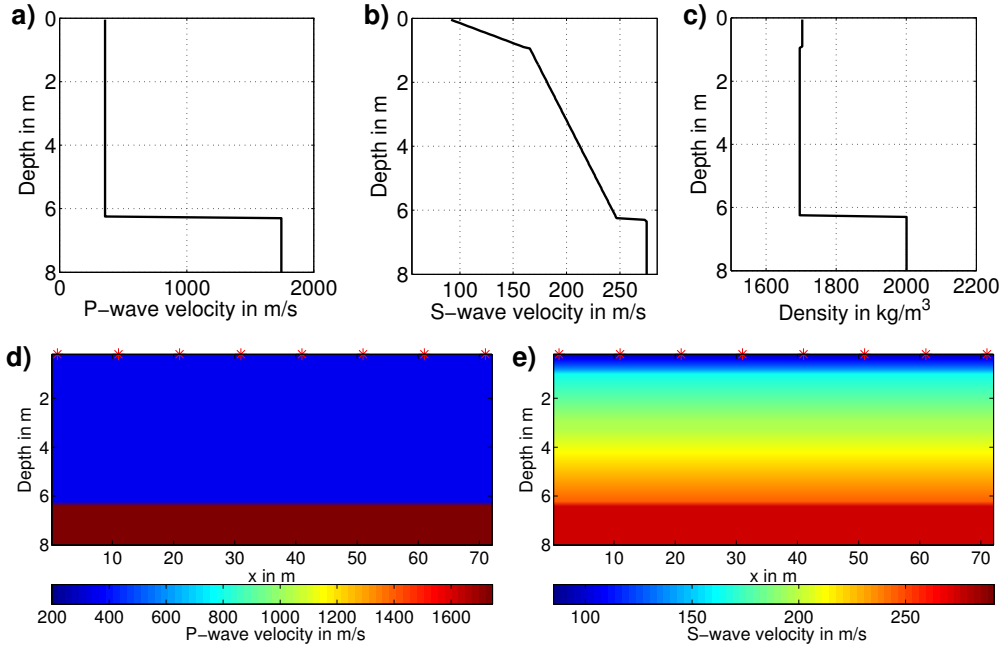

Figure 1: True model used in the reconstruction tests. a) shows the P-wave velocity model, b) the S-wave velocity model and c) the density model. d) and e) display again the P-wave velocity model and the S-wave velocity where the velocities are color coded. The red stars mark the positions of the eight sources used in the reconstruction tests. d) and e) do not show the whole model used for the simulations (CPML boundaries as well as the lower part of the part of the models are cut off).

We apply frequency filtering during the inversion. We start with a fourth order Butterworth lowpass filter at 10 Hz and increase the bandwidth up to 70 Hz in steps of 5 Hz. The gradients have high amplitudes around the sources. Therefore, they must be strongly damped in these regions. However, in shallow seismics we also want to invert the shear wave velocity structure near the sources. Therefore, we precondition the gradients of each shot before summing them to obtain an update at the shot positions in the final gradient. As preconditioning taper we use a circular taper around the current shot position with a radius of 3.0 m and an increasing amplitude from the center to the boundary. After each iteration step the models are smoothed with a 2D median filter with a filterlength of 0.6 m.

The number of iteration steps in the different reconstruction tests varies between 195 and 210 iterations and the computing time is around 26 hours on 4 CPUs for each test.

RESULTS OF RECONSTRUCTION TESTS

In this section we present the results of the reconstruction tests. In all tests we use a linear gradient for S-wave velocity as well as density as initial model. The gradients start with the correct value of the corresponding model parameter at the surface and increase linearly up to 9 m depth where they reach the correct values in the halfspace of the corresponding model parameter. The model used for P-wave velocity varies between the reconstruction tests. Although we also invert for density we show only P and S-wave velocity models in the following. The reconstruction of the density model fails because it is not well constrained by the observed data.

Test 1: P-wave velocity model fixed, true P-wave velocity model

In the first reconstruction test we only invert for S-wave velocity and density and use the true P-wave velocity model as fixed model in the inversion (Figure 2b and d). The result for the S-wave velocity model

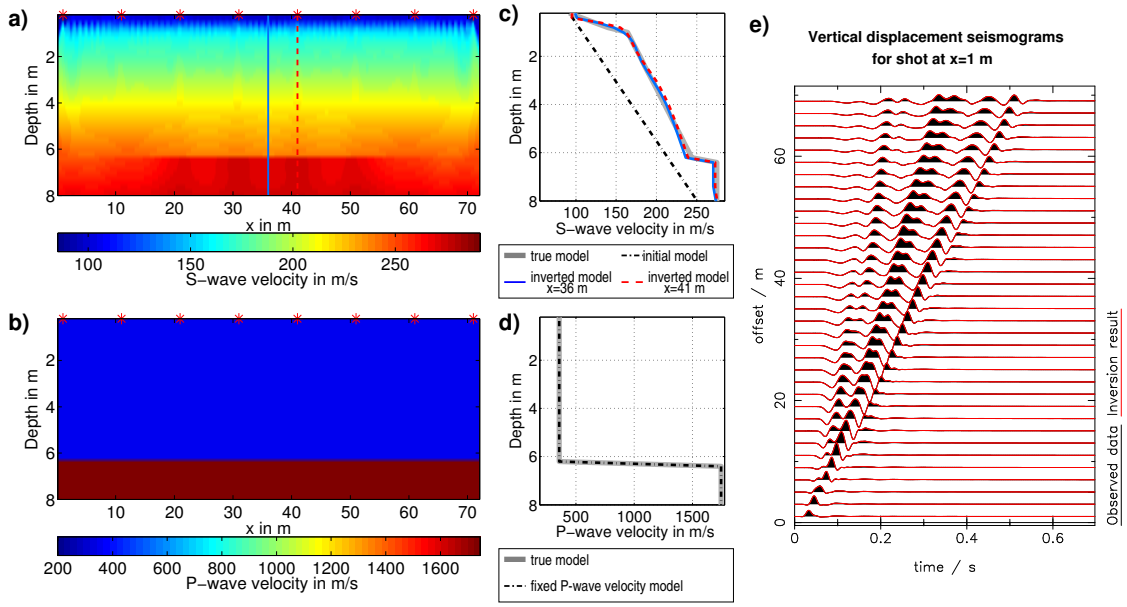

Figure 2: Results of reconstruction test 1. a) shows the obtained S-wave velocity model. The blue and the red dashed lines mark the position of the two vertical profiles shown in c) in comparison to the true S-wave velocity model (thick grey line) and the initial S-wave velocity model (dash-dotted black line). b) displays the fixed P-wave velocity model which coincides with the true P-wave velocity model and is used throughout the inversion. d) shows a comparison of vertical velocity profiles of the true P-wave velocity model and the P-wave velocity model used in the inversion. e) shows the vertical displacement seismograms of the left shot at x=1 m for the observed data (black) and the final inversion result (red). Not all traces are shown. The traces are not trace normalized but they are multiplied by an offset dependent factor of $\left(\frac{r}{\mathrm{m}}\right)^{0.7}$.

is shown in Figure 2a. Figure 2c shows two vertical velocity profiles (continuous blue and dashed red line) in comparison to the true model (thick grey line) and the initial model (dash-dotted black line). The location of the profiles is marked by the two lines in Figure 2a. The reconstruction of the S-wave velocity model is almost perfect in this test. The resulting structure is nearly one dimensional and all characteristics of the S-wave velocity model (both gradients as well as the small discontinuity) are reconstructed successfully. Figure 2e shows displacement seismograms of the left shot at x=1 m for the vertical component. The observed data are plotted in black and the seismograms obtained with the final subsurface model inferred from the data are plotted in red. The two wavefields fit each other very well and the final data misfit for all shots and both components is E_{final}=0.001 (calculated with Equation (1)) and is therefore very small (initial data misfit of $E_{initial}$=1.06).

Test 2: P-wave velocity model fixed, P-wave velocity model derived from first arrival travel times

When we want to apply FWI to recorded data we do not have the true P-wave velocity model and cannot use it within an inversion. Therefore, the first test is quite unrealistic. A very simple approach to obtain a P-wave velocity model from the data is a P-wave refraction analysis. We apply such an analysis to the simulated observed data of the two outermost shots in the model (at x=1 m and x=71 m) and obtain the P-wave velocity model shown in Figure 3b by averaging both results. This model is used as fixed P-wave velocity model in the second reconstruction test. Figure 3d shows the difference between the true P-wave velocity model (thick grey line) and the model used in the inversion (dash-dotted black line). Using the wrong P-wave velocity model and keeping it fixed in the inversion causes strong artefacts in the S-wave velocity model (Figure 3a and c). We observe a periodic pattern which coincides with the source positions and especially the strong gradient in the topmost metre can not be reconstructed in the inversion. However,

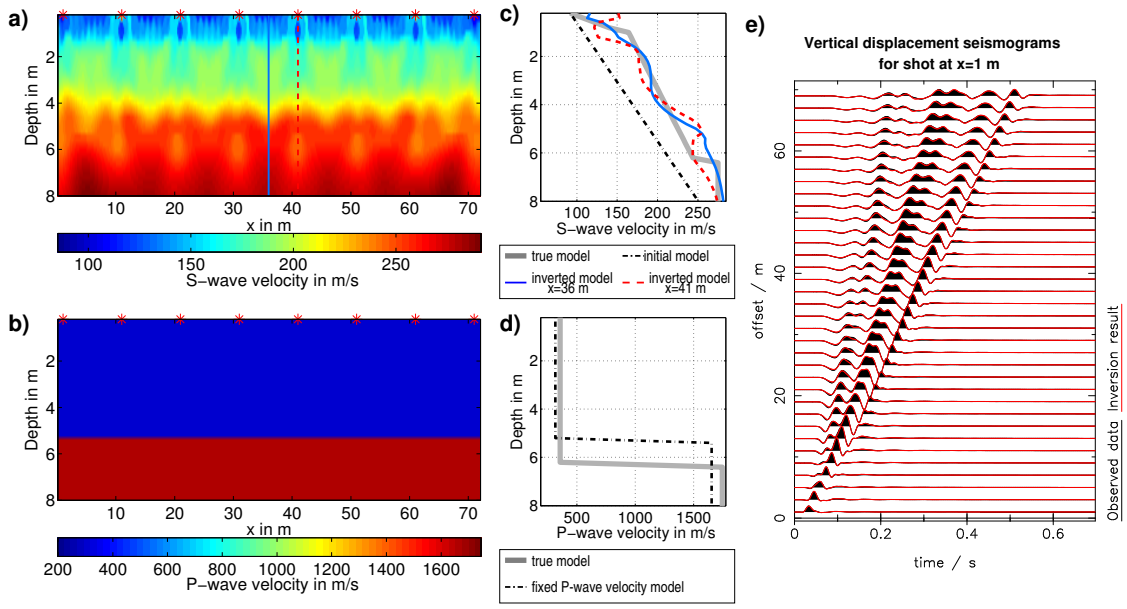

Figure 3: Results of reconstruction test 2. a) shows the obtained S-wave velocity model. The blue and the red dashed lines mark the position of the two vertical profiles shown in c) in comparison to the true S-wave velocity model (thick grey line) and the initial S-wave velocity model (dash-dotted black line). b) displays the fixed P-wave velocity model which is used throughout the inversion. d) shows a comparison of vertical velocity profiles of the true P-wave velocity model (thick grey line) and the P-wave velocity model used in the inversion (dash-dotted black line). e) shows the vertical displacement seismograms of the left shot at x=1 m for the observed data (black) and the final inversion result (red). Not all traces are shown. The traces are not trace normalized but they are multiplied by an offset dependent factor of $\left(\frac{r}{\mathrm{m}}\right)^{0.7}$.

the final data misfit of 0.018 is relatively small compared to the strong artefacts in the S-wave velocity model (inital data misfit $E_{initial}$=1.01).

Test 3: P-wave velocity model inverted, initial P-wave velocity model derived from first arrival travel times

In our third test we use again the P-wave velocity model which is derived from the observed data by an analysis of the direct and refracted P-wave onsets. In contrast to our second test we now also invert for the P-wave velocity model. The final S-wave velocity model and P-wave velocity model are shown in Figure 4a and b. Figure 4c and d show vertical velocity profiles for the S-wave and P-wave velocity model, respectively, in comparison to the true velocity models and the initial velocity models. The S-wave velocity model is reconstructed quite well down to approximately 4.5 m depth. Below we observe a small discontinuity in approximately 5.0 m depth which is quite similar to the discontinuity in 6.3 m depth in the true S-wave velocity model. The small discontinuity in the obtained S-wave velocity model coincides in depth with the large discontinuity in the initial P-wave velocity model. This discontinuity is not changed during the inversion and is still present in the P-wave velocity model inferred from the data. Thus we observe a clear bias of the P-wave velocity model on the reconstruction of the S-wave velocity model in this test. The P-wave velocity model is only changed in the upper layer during the FWI. The fact that the depth of the discontinuity in the P-wave velocity model is not adjusted during the FWI is possibly caused by the small bandwidth of the observed data (up to 70 Hz). The low frequent P-waves maybe do not constrain the depth of the discontinuity accurate enough. In comparison to test 2 the final data misfit decreases again to 0.004 (initial data misfit $E_{initial}$=1.01).

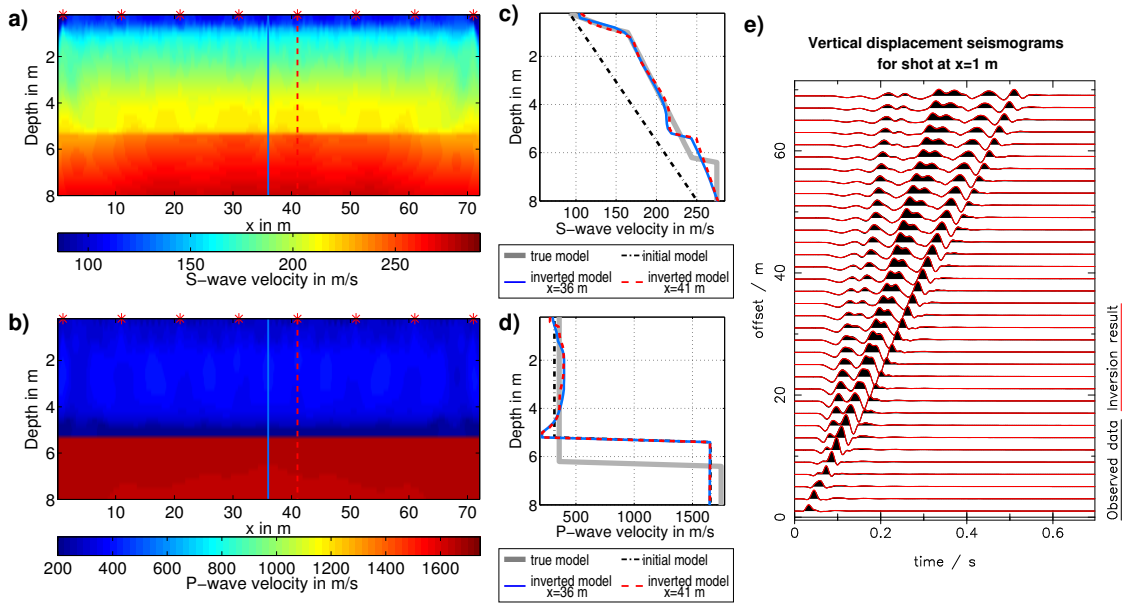

Figure 4: Results of reconstruction test 3. a) and b) show the obtained S-wave velocity model and P-wave velocity model, respectively. The blue and the red dashed lines mark the position of the vertical profiles shown in c) and d) in comparison to the true velocity models (thick grey line) and the initial velocity models (dash-dotted black line). e) shows the vertical displacement seismograms of the left shot at x=1 m for the observed data (black) and the final inversion result (red). Not all traces are shown. The traces are not trace normalized but they are multiplied by an offset dependent factor of $\left(\frac{r}{\mathrm{m}}\right)^{0.7}$.

Test 4: P-wave velocity model inverted, linear gradient as initial P-wave velocity model

We observed in the third test that FWI is not able to shift the strong discontinuity in the P-wave velocity which is present in the inital model. Therefore, in our last test we use a linear gradient as initial P-wave velocity model in the inversion (see dash-dotted black line in Figure 5d). We again invert for all three elastic parameters (P-wave velocity, S-wave velocity and density). The inversion results are shown in Figure 5. The initial P-wave velocity model is only changed in the first two metres of the subsurface and we were not at all able to reconstruct the true P-wave velocity model, in particular there is no sign of a halfspace and a discontinuity on top of the halfspace in the final model (Figure 5b and d). The S-wave velocity model again shows a periodic pattern which coincides with the source positions. However, we do not observe huge artefacts as in test 2 where we used a wrong P-wave velocity model as fixed P-wave velocity model in the inversion. We can reconstruct the two gradients in the S-wave velocity model with only slight deviations from the true model. We are not able to reconstruct the discontinuity at 6.3 m depth. However, in contrast to test 3 we also do not observe an artificial discontinuity at a wrong depth. The final data misfit in this inversion of 0.088 is quite high compared to the final data misfit in the other tests (initial data misfit in this test is $E_{initial}$=1.14). Although the fit of the fundamental mode is again quite well (Figure 5e) the fit of the P-waves and the higher modes of the Rayleigh waves is bad because the inversion was not at all able to reconstruct the P-wave velocity model.

CONCLUSION AND OUTLOOK

In our tests we observe a significant bias of the P-wave velocity model on the reconstruction of the S-wave velocity model. It is desirable to use a P-wave velocity model which is as similar as possible to the true P-wave velocity model to obtain an accurate S-wave velocity model. However, discontinuities in the initial P-wave velocity model can lead to artificial discontinuities in the S-wave velocity model inferred from the data. Furthermore, in case of using a wrong P-wave velocity model in the inversion it should not be

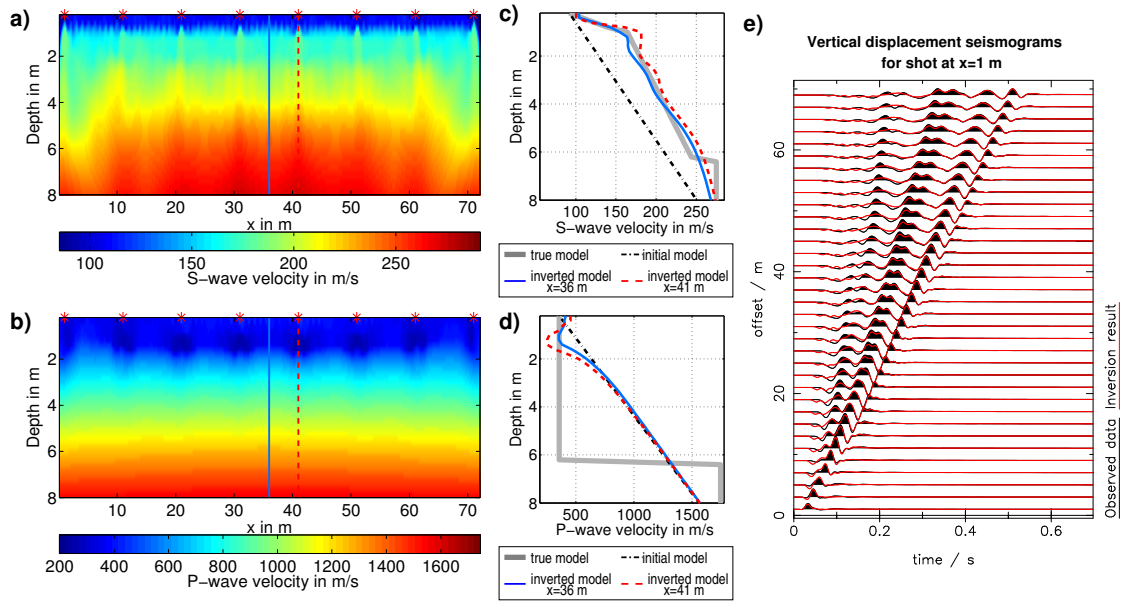

Figure 5: Results of reconstruction test 4. a) and b) show the obtained S-wave velocity model and P-wave velocity model, respectively. The blue and the red dashed lines mark the position of the vertical profiles shown in c) and d) in comparison to the true velocity models (thick grey line) and the initial velocity models (dash-dotted black line). e) shows the vertical displacement seismograms of the left shot at x=1 m for the observed data (black) and the final inversion result (red). Not all traces are shown. The traces are not trace normalized but they are multiplied by an offset dependent factor of $\left(\frac{r}{\mathrm{m}}\right)^{0.7}$.

fixed because this can cause strong artefacts in the obtained S-wave velocity model. In our tests it was not possible to invert the P-wave velocity model satisfactorily. In principle, FWI should be able to reconstruct quite accurate P-wave velocity models. Therefore, further tests should investigate, how to improve the inversion of this model parameter. As the P-waves (wich mainly constrain the P-wave velocity model) have relatively small amplitudes in comparison to the surface waves they do not contribute in the same extent to the misfit as the Rayleigh waves. Therefore, maybe time windowing can help to firstly invert the P-waves in a FWI to obtain an accurate P-wave velocity model which can be used afterwards in an inversion of the whole dataset for the reconstruction of the S-wave velocity model.

ACKNOWLEDGMENTS

The work was performed within the project TOAST which is part of the GEOTECHNOLOGIEN program, funded by the German Ministry of Education and Research (BMBF) and German Research Foundation (DFG), Grant/Förderkennzeichen 03G0752. This work was also kindly supported by the sponsors of the *Wave Inversion Technology (WIT) Consortium*, Germany. We also thank Daniel Köhn for providing the 2D elastic FWI code.

REFERENCES

Bachrach, R., Dvorkin, J., and Nur, A. M. (2000). Seismic velocities and poisson's ratio of shallow unconsolidated sands. *Geophysics*, 65(2):559–564.

Bohlen, T. (2002). Parallel 3-D viscoelastic finite difference seismic modelling. *Computers & Geosciences*, 28:887–899.

Choi, Y. and Alkhalifah, T. (2012). Application of multi-source waveform inversion to marine streamer data using the global correlation norm. *Geophysical Prospecting*, 60:748–758.

Forbriger, T. (2003). Inversion of shallow-seismic wavefields: Part I and II. *GJI*, 153(3):719–752.

Köhn, D. (2011). Time domain 2D elastic full waveform tomography. *Dissertation, Kiel, Christian-Albrechts-Universität zu Kiel*.

Mora, P. (1987). Nonlinear two-dimensional elastic inversion of multioffset seismic data. *Geophysics*, 52(9):1211–1228.

Robertsson, J. O. A., Blanch, J. O., and Symes, W. W. (1994). Viscoelastic finite-difference modeling. *Geophysics*, 59(9):1444–1456.

Romdhane, G., Grandjean, G., Brossier, R., Rejiba, F., Operto, S., and Virieux, J. (2011). Shallow-structure characterization by 2D elastic full-waveform inversion. *Geophysics*, 76(3):R81–R93.

Tarantola, A. (1988). Theoretical background for the inversion of seismic waveforms, including elasticity and attenuation. *Pure Appl. Geophys.*, 128(1-2):365–399.

Tran, K. T. and McVay, M. (2012). Site characterization using gauss-newton inversion of 2-D full seismic waveform in the time domain. *Soil Dyn. Earthq. Eng.*, 43:16–24.